Hydrol. Earth Syst. Sci. Discuss., 3, 2853–2897, 2006
www.hydrol-earth-syst-sci-discuss.net/3/2853/2006/

Hydrology and Earth System Sciences Discussions

Papers published in *Hydrology and Earth System Sciences Discussions* are under open-access review for the journal *Hydrology and Earth System Sciences*

Temporal dynamics of hydrological threshold events

G. S. McGrath[1], C. Hinz[1], and M. Sivapalan[2]

[1]School of Earth and Geographical Sciences, University of Western Australia, Crawley, Australia
[2]Departments of Geography & Civil & Environmental Engineering, University of Illinois at Urbana-Champaign, USA

Received: 14 July 2006 – Accepted: 1 September 2006 – Published: 15 September 2006

Correspondence to: C. Hinz (chinz@cyllene.uwa.edu.au)

Abstract

The episodic nature of hydrological flows such as surface runoff and preferential flow is a result of the nonlinearity of their triggering and the intermittency of rainfall. In this paper we examine the temporal dynamics of threshold processes that are triggered by either an infiltration excess (IE) mechanism when rainfall intensity exceeds a specified threshold value, or a saturation excess (SE) mechanism governed by a storage threshold. We analytically derive probabilistic measures of the time between successive events in each case, and in the case of the SE triggering, we relate the statistics of the time between events to the statistics of storage and the underlying water balance. In the case of the IE mechanism, the temporal dynamics of flow events is shown to be simply scaled statistics of rainfall timing. In the case of the SE mechanism the time between events becomes structured. With increasing climate aridity the mean and the variance of the time between SE events increases but temporal clustering, as measured by the coefficient of variation (CV) of the inter-event time, reaches a maximum in deep stores when the climatic aridity index equals 1. In very humid and also very arid climates, the temporal clustering disappears, and the pattern of triggering is similar to that seen for the IE mechanism. In addition we show that the mean and variance of the magnitude of SE events decreases but the CV increases with increasing aridity. The CV of inter-event times is found to be approximately equal to the CV of the magnitude of SE events per storm only in very humid climates with the CV of event magnitude tending to be much larger than the CV of inter-event times in arid climates. In comparison to storage the maximum temporal clustering was found to be associated with a maximum in the variance of soil moisture. The CV of the time till the first saturation excess event was found to be greatest when the initial storage was at the threshold.

1 Introduction

Hydrological processes which result from highly nonlinear, threshold like mechanisms include interception (Savenije, 2004; Crockford and Richardson, 2000), hillslope out flow via subsurface pathways (Whipkey, 1965), preferential flow (Beven and Germann, 1982), Hortonian overland flow, saturation excess overland flow (Dunne, 1978), and erosion (Fitzjohn et al., 1998) amongst others. These processes occur episodically due to their threshold-like response to intermittent rainfall. We define episodic processes as short lived discrete events that are not triggered for every single rainfall event.

There is much hydrological theory and modelling devoted to the prediction of the flux of water and solutes in soils at the field and larger scales (Bresler and Dagan, 1982; Roth and Jury, 1993; Jarvis et al., 1994) and while our understanding of the mechanics of many hydrological processes is reasonably well developed (Dunne, 1978; Parlange and Hill, 1976; Beven and Germann, 1982), hydrological prediction of the fluxes still suffers from high uncertainty (Zak and Beven, 1999; Minasny and McBratney, 2002).

The dynamics of episodic hydrological events driven by rainfall can also be expressed in terms of the timing of their triggering. However, this aspect of the dynamics is poorly understood. Given the difficulty in predicting the fluxes accurately, there is a need to quantify the temporal dynamics of such processes in terms of storm and climate properties. Additionally there is as yet little understanding of the relationship between the fluxes and the timing of the runoff events which are clearly linked through soil moisture storage. Improved understanding with respect to the last two points are the main objectives of the work presented here.

In this paper we introduce a generic analysis, quantifying how the temporal dynamics of these episodic events emerges from the rainfall signal as a result of the nonlinearity of the intervening hydrological process. This nonlinear or threshold filtering is assessed by the statistical properties of the time it takes to trigger an event for the first time and the time between successive events. We then go on to compare how the statistical properties of runoff fluxes and the timing of the triggering of events vary with respect to

storm properties and the climate setting.

1.1 Threshold triggers

The initiation of fast flow such as surface runoff and rapid preferential flow is either caused by infiltration excess or a storage (saturation) excess mechanism. For example macropore flow can be triggered at the soil surface by high rainfall intensities that are in excess of the infiltration capacity of the soil matrix, while surface runoff occurs when infiltration capacity of both the soil matrix and the macropores are exceeded (Beven and Germann, 1982). Alternatively, macropore flow can be initiated when the soil matrix becomes saturated allowing water to move from the matrix into large voids (Beven and Germann, 1982; Simunek et al., 2003).

Other flow processes are similarly triggered by thresholds in storage and / or storm amount. These include various types of preferential flow (Dekker et al., 2001; Bauters, 2000; Wang et al., 1998; Kung, 1990; Haria et al., 1994; Heppell et al., 2002; Beven and Germann, 1982), canopy interception (Crockford and Richardson, 2000; Zeng et al., 2000), and hillslope outflow through subsurface flow pathways (Whipkey, 1965; Mosley, 1976; Uchida et al., 2005; Tromp-van Meerveld and McDonnell, 2006).

The temporal dynamics of preferential flow triggering due to between-storm and within-storm rainfall variability has been previously explored via the numerical simulation approach using synthetic rainfall time series (Struthers et al., 2006a,b). Struthers et al. (2006b) were able to relate the pdf and specific statistical characteristics of the storm inputs to statistical properties and pdfs of runoff magnitude and timing of the runoff events. The analysis was not able to separate the contributions of the various runoff mechanisms to the statistical properties of the resulting temporal flow dynamics.

In this article we examine two extreme but simple conceptualisations of nonlinear flow triggering: the first, an infiltration excess mechanism, is based on a threshold rainfall intensity (Kohler et al., 2003) neglecting any soil moisture storage controls. The second mechanism represents the other, opposite extreme, a saturation excess mechanism, based upon a threshold storage, depending only on the storm amount and

not its intensity. This mechanism captures the carry over of storage from one rainfall event to the next. As a result there is an enhanced probability that a second flow event will occur shortly after a flow event has just occurred because storage is more likely to be nearer the threshold in this interval. We hypothesise that temporal clustering of saturation excess events is a characteristic of the rainfall filtering, which means that multiple events occur in short periods of time separated by longer event-free intervals.

1.2 Outline

The paper begins with a brief overview of the simple models of rainfall adopted for this analysis. Based upon this we derive analytically the statistics of the time between threshold events for infiltration excess and saturation excess mechanisms, and for saturation excess we also present existing and newly derived statistics of the runoff flux based upon the original work of Milly (1993, 2001). Finally, we explore the results in the context of storm properties and the climate setting.

2 Rainfall models

For modelling purposes we adopt simple stationary descriptions of rainfall without any seasonal dependence. Storms are characterised only by three parameters, their total depth h [L], a maximum within-storm intensity $I_{\max}$ [L/T], and an inter-storm time t_b [T]. Storms are considered to be instantaneous events, independent of one another, therefore satisfying the Poisson assumption as used commonly in hydrology (Rodriguez-Iturbe et al., 1999; Milly, 1993). Such an assumption is considered valid at near daily time scales (Rodriguez-Iturbe and Isham, 1987). This implies that the random time between storms, the inter-storm time, that results is described by an exponential probability density function (pdf) (Rodriguez-Iturbe et al., 1999):

$$g_{Tb}[x] = \frac{1}{\bar{t}_b} e^{-x/\bar{t}_b} \tag{1}$$

which is fully characterised by its mean $\bar{t}_b$ [T]. Storm depths are also assumed to follow an exponential pdf $f_H[h]$ with a mean γ [L]. The maximum within-storm rainfall intensity is also considered to be exponentially distributed with a mean of ς [L/T].

3 Statistics of temporal dynamics

Based on the rainfall signal and soil properties we would like to quantify the probability that a given flow event, involving the exceedance of some kind of threshold, occurs. We use the time between events as the random variable that characterises this event probability. This concept is illustrated for a rainfall intensity threshold (Fig. 1a) and a soil moisture storage threshold (Fig. 1b). The random time to reach these thresholds for the first time is referred to as a first passage time (FPT) denoted as τ_1, and the time between flow events is referred to as the inter-event time (IET) denoted as τ_2 and τ_3 in Fig. 1a and Fig. 1b. In the case of infiltration excess runoff, a flow event is triggered when the maximum rainfall intensity within a storm exceeds the infiltration capacity I_ξ. In contrast, when the soil water storage reaches a critical capacity a saturation excess event is deemed to have been triggered.

To quantify the probability density functions of the first passage times and the inter-event times, we use the first four central moments. For completeness we define the moments in this section and will derive analytical expressions for them in Sect. 5.2 and Appendix A. The mean T_μ [T] and the kth central moment μ_k of the random variable τ are related to the pdf $g_T[\tau]$ by the following (Papoulis, 2001):

$$T_\mu = E[\tau] = \int_{-\infty}^{\infty} \tau \, g_T[\tau] \, \mathrm{d}\tau \tag{2}$$

$$\mu_k = E\left[(\tau - E[\tau])^k\right] = \int_{-\infty}^{\infty} (\tau - T_\mu)^k \, g_T[\tau] \, \mathrm{d}\tau \tag{3}$$

for integers $k \geq 2$, where $E[\ ]$ denotes the expectation operator. In addition to the mean and the variance $T_{\sigma^2} = \mu_2$ $\left[\mathrm{T}^2\right]$, we will also use the dimensionless statistic, the coefficient of variation $T_{cv} = \sqrt{T_{\sigma^2}} / T_\mu$ [−], the ratio of the standard deviation to the mean, which gives a measure of the variability relative to the mean; the coefficient of skewness $T_\varepsilon = \mu_3 / \mu_2^{3/2}$ [−], which describes the asymmetry of the probability distribution, where positive values indicate that the distribution has a longer tail towards larger values than smaller values; and the coefficient of kurtosis $T_\kappa = \mu_4 / \mu_2^2 - 3$ [−], where positive values indicate a more peaked distribution, in comparison to a normally distributed variable, and "fatter tails" i.e. an enhanced probability of extreme values (Papoulis, 2001).

In order to compare the statistical properties of flow event triggers with the rainfall signal, we summarise here the rainfall in terms of IET statistics. The idea here is to compare and contrast inter-storm and inter-event statistics for the various threshold driven processes. Events which are temporally independent of one another, such as our model rainfall, have an exponential IET pdf. Table 1 lists the statistics for the inter-storm time.

A property of the exponential distribution, which describes the inter-event time of independent events, is that the mean is equal to the standard deviation, and therefore the coefficient of variation is equal to 1. The coefficient of variation of the inter-event time T_{cv} is often used to distinguish temporally clustered and unclustered processes (Teich et al., 1997). Temporal clustering is said to occur when $T_{cv} > 1$, a $T_{cv} = 0$ indicates no variability and exactly regular events, while a $T_{cv} < 1$ may indicate a quasi-periodic process (Godano et al., 1997; Wood et al., 1995).

4 Infiltration excess inter-event time statistics

Here we assume for simplicity that the infiltration capacity I_ξ is constant (Kohler et al., 2003), and therefore soil moisture controls on the infiltration capacity are considered

insignificant. This approach provides an extreme contrast to the saturation excess mechanism considered. It may actually represent well more extreme rainfall where the antecedent soil moisture has little impact on event triggering. For example Heppell et al. (2002) classified preferential flow events in a clay loam soil as antecedent soil moisture limited and non-antecedent limited events. The non-antecedent limited events were related to storms where the maximum within-storm rainfall intensity was much larger than the mean storm intensity.

This constant threshold filtering is the same as the rainfall filtering described in Rodriguez-Iturbe et al. (1999) in the context of the soil water balance. They showed that a threshold filtering of Poisson rainfall resulted in a new Poisson process with an event rate equal to the storm arrival rate multiplied by the probability of exceeding the threshold (Rodriguez-Iturbe et al., 1999). For the infiltration excess trigger, when the maximum within-storm rainfall intensity $I_{\max}$ is exponentially distributed with mean ς the probability that $I_{\max} > I_\xi$ is equal to $e^{-I_\xi/\varsigma}$ and therefore the resulting mean time between threshold intensity events is equal to $T_\mu^I = \bar{t}_b e^{I_\xi/\varsigma}$. Table 1 lists the IET statistics that result for this process.

A soil with an infiltration capacity twice the mean maximum within-storm rainfall intensity results in a mean IET which is e^2 times longer than the mean inter-storm time $\bar{t}_b$, and a variance e^4 times greater than the inter-storm time variance $\bar{t}_b^2$. The higher central moments remain unchanged. The threshold driven infiltration excess filtering therefore results in temporal dynamics that are statistically the same as the rainfall's, but scaled by a factor related to the single event probability of exceeding the threshold. This is illustrated in Fig. 2a, which is a semi-log plot of an example infiltration excess IET pdf, corresponding to the above example, shown in comparison to the rainfall IET pdf.

5 Saturation excess filtering

In this section saturation excess is described on the basis of Milly's (1993) nonlinear storage-runoff model. Milly used this model to describe the impact of rainfall intermittency and soil water storage on runoff generation at catchment scales, and which he successfully used to capture much of the spatial variability in the annual water balance in catchments across much of continental USA (Milly, 1994). We use this minimalist framework to model the triggering of runoff by the exceedance of a threshold value of storage. We first review his analytical results for the statistics of soil moisture storage and the mean water balance components. We then go on to derive from these results the variance of the saturation excess runoff flux on a per storm basis. We will later relate these statistics to those of the temporal dynamics of saturation excess triggering.

5.1 Storage and the water balance

Milly's (1993) water balance model is represented in terms of a simple bucket with a fixed storage capacity w_0 [L] which wets in response to random storm events and dries in the inter-storm period, of random duration, due to a constant evaporative demand E_m [L/T]. The threshold soil moisture (s_ξ=1 [-]) for flow initiation is assumed to have been reached when the store is filled to capacity. Any excess rainfall becomes saturation excess. The resulting stochastic balance equation for water storage s [-] (a dimensionless storage normalised by w_0) is:

$$\frac{\mathrm{d}s}{\mathrm{d}t} = -L\,[s] + F\,[s,t] \tag{4}$$

where t [T] denotes time, $L\,[s]$ $\left[\mathrm{T}^{-1}\right]$ the (normalised by w_0) evaporative losses from storage. $F\,[s,t]$ [−] denotes instantaneous random infiltration events (normalised by w_0), occurring at discrete times t_i. Infiltration is limited by the available storage capacity i.e. $F\,[s,t_i] = \min\left[1-s_i^-, h_i/w_0\right]$, where s_i^- [−] denotes the antecedent soil moisture

and h_i [L] the random storm depth. Evaporation losses are given by:

$$L\,[s] = \begin{cases} 0 & \text{for} \quad s = 0 \\ \frac{E_m}{w_0} & \text{for} \quad 0 < s \leq 1 \end{cases} \tag{5}$$

In this article we largely consider the transformation of Eq. (4) directly into the statistical properties of inter-event times, however we discuss briefly here how to numerically simulate a storage time series. This is done in part to help explain the conceptualisation of the process as well as to describe how we generated example time series presented in Sect. 6.3.1. Simulation involves generating a random inter-storm time t_b and a subsequent storm depth h from their respective probability distributions. Storage at any time t in the inter-storm period can be calculated from $s\,[t] = \max\left[0, s_0 - E_m(t-t_0)/w_0\right]$, where t_0 is the time of the last storm when soil moisture was s_0. At the end of the inter-storm time $t_i = t_0 + t_b$ storage immediately prior to the storm is given by s_i^-. Storage increases from s_i^- to $s_i^+ = \min\left[1, s_i^- + h/w_0\right]$ due to the storm also at a time t_i. This occurs as an instantaneous event with storage taking on two separate values immediately either side of time t_i. The simulation is then continued with s_i^+ as the new s_0 and so on.

From the above model and the characteristics of rainfall presented before, two similarity parameters can be defined: the supply ratio $\alpha = w_0/\gamma$, the ratio of storage capacity to mean storm depth, and the demand ratio $\beta = w_0/\left(E_m \bar{t}_b\right)$, the ratio of storage capacity to mean potential inter-storm evaporation (Milly, 1993). When α=0 the rainfall supply is infinitely larger than storage capacity and when α=∞ the supply is negligible compared to the amount in storage at capacity. Similarly β=0 indicates infinite evaporative demand and β=∞ negligible demand relative to the storage capacity. Typically one could expect the parameters to range from about 1 to 100 depending upon the process considered. For example a thin near surface water repellent layer with 10 mm of storage could have realistic α values of 1 to 10 depending upon the mean storm depth. Runoff controlled by storage throughout the rooting depth may have much larger values

(Milly, 2001).

The ratio $AI=\left(E_m\bar{t}_b\right)/\gamma=\alpha/\beta$ defines the relative balance between mean potential inter-storm evaporation and the mean storm depth and is otherwise known as the climatic aridity index. An $AI<1$ describes a humid climate, $AI>1$ an arid climate and $AI=1$ defines equal mean rainfall and mean potential evaporation.

Milly (1993) derived the pdf of water storage in the form of two derived distributions of storage: one for a time immediately before a storm f_{S^-}, the antecedent storage pdf, and one immediately after a storm f_{S^+}. The pdf for storage for all times f_S, that resulted from that analysis was found to be equal to f_{S^-} (Milly, 2001). This was essentially because storms were modelled as instantaneous events, with no duration, and the expected arrival time of the next storm was a memoryless Poisson process. The pdf of f_S is given by:

$$f_S = p\beta\, e^{(\alpha-\beta)s} + q\delta\,[s] \tag{6}$$

where δ denotes the Dirac delta function, p describes the probability storage is at capacity (s=1), and q the probability that the soil is dry (s=0) and are given by:

$$p = \frac{\alpha-\beta}{\alpha\, e^{\alpha-\beta}} \qquad q = \frac{\beta-\alpha}{\beta\, e^{\beta-\alpha}-\alpha}$$

The resulting mean S_μ and variance S_{σ^2} of storage are given by Eq. (7) and Eq. (8) respectively (Milly, 2001):

$$S_\mu = \frac{1}{\alpha-\beta} + \frac{1+\beta\, e^{\beta-\alpha}}{\beta\, e^{\beta-\alpha}-\alpha} \tag{7}$$

$$S_{\sigma^2} = \frac{1}{(\alpha-\beta)^2} - \frac{1+(\alpha+2)\,\beta\, e^{\beta-\alpha}}{\left(\beta\, e^{\beta-\alpha}-\alpha\right)^2} \tag{8}$$

Based on the definition of the expected value of a function $g\,[x]$ of a random variable x , with a known pdf $f_X\,[x]$ (Papoulis, 2001):

$$E\,[g\,[x]] = \int_{-\infty}^{\infty} g\,[x]\, f_X\,[x]\,\mathrm{d}x \tag{9}$$

Milly (1993) derived the mean actual evaporation E_a [L] per inter-storm period via:

$$\frac{E_a}{\gamma} = \frac{w_0}{\gamma}\int_{0^-}^{1} L\,[s]\; f_S\,[s]\;\mathrm{d}s = 1 - \frac{\alpha-\beta}{\alpha\, e^{\alpha-\beta}-\beta} \tag{10}$$

where the 0^- is used to denote inclusion of the probability that $s = 0$.

From mass balance considerations Milly (1993) then determined the mean runoff per storm Q_μ [L] as follows:

$$\frac{Q_\mu}{\gamma} = 1 - \frac{E_a}{\gamma} = \frac{\alpha-\beta}{\alpha e^{\alpha-\beta}-\beta} \tag{11}$$

Extending such analysis, we derive here for the first time the variance of flux per storm event Q_{σ^2} $\left[\mathrm{L}^2\right]$ which we calculate from the definition of the variance of a function of two random variables $G\,[x,y]$ which have a joint pdf $f_{XY}\,[x,y]$ (Papoulis, 2001) which is given by:

$$E\left[\left(G\,[x,y]-E\,[G\,[x,y]]\right)^2\right] = \int_{-\infty}^{\infty}\int_{-\infty}^{\infty}\left(G\,[x,y]-E\,[G\,[x,y]]\right)^2 f_{XY}\,[x,y]\;\mathrm{d}x\;\mathrm{d}y \tag{12}$$

The magnitude of saturation excess generated on a single event Q_i is given by:

$$Q_i\left[h_i, s_i^-\right] = \max\left[0, h_i - w_0\left(1-s_i^-\right)\right] \tag{13}$$

which depends upon the two random variables, storm depth h_i and the antecedent soil moisture s_i^- . As the pdf of soil moisture immediately prior to a rainfall event f_{S^-}

is equivalent to the pdf of soil moisture f_S (Eq. 6) in this instance (Milly, 2001) and as h and s^- are independent random variables we can apply Eq. (12) and the condition Eq. (13) to the calculation of the saturation excess runoff variance Q_{σ^2} by the following:

$$\frac{Q_{\sigma^2}}{\gamma^2} = \int_{0^-}^{1}\int_{w_0(1-s)}^{\infty}\left(\frac{w_0}{\gamma}\left(\frac{h}{w_0}-1+s\right)-\frac{Q_\mu}{\gamma}\right)^2 w_0 f_H[h]\, f_S[s]\ \mathrm{d}h\,\mathrm{d}s \quad + \int_{0^-}^{1}\int_{0}^{w_0(1-s)}\left(-\frac{Q_\mu}{\gamma}\right)^2 f_H[h]\, w_0 f_S[s]\ \mathrm{d}h\,\mathrm{d}s = \frac{(\alpha-\beta)\ \left(2\alpha\, e^{\alpha-\beta}-\alpha-\beta\right)}{\left(\alpha\, e^{\alpha-\beta}-\beta\right)^2} \quad (14)$$

5.2 Statistics of saturation excess timing

For the type of stochastic process modelled by Milly (1993) (a shot noise process), Laio et al. (2001) and Masoliver (1987) provided derivations for the mean time to reach a threshold for the first time. This methodology was subsequently applied to describe the mean duration of soil moisture persistence between upper and lower bounds in order to investigate vegetation water stress (Ridolfi et al., 2000).

The mean first passage time describes the expected waiting time till an event, of which the mean inter event time is a special case. However the temporal dynamics also consists of the variability about this mean behaviour, therefore in Appendix A we present, for the first time, an extension of the derivation for the mean first passage time (Laio et al., 2001) giving a general solution to the higher moments of the FPT, such as the variance.

Using Eqs. (A5), (A13) and (A10), with n=1 , T_0=1 and L [s] as given by Eq. (5) we can derive the mean time $T_\mu^s\left[s_0, s_\xi\right]$ till an arbitrary threshold storage s_ξ is reached for

the first time, when the initial storage was $s_0 \leq s_\xi$ as:

$$\frac{T_\mu^s\left[s_0, s_\xi\right]}{\bar{t}_b} = \frac{\alpha\left(\alpha e^{s_\xi(\alpha-\beta)}-\beta e^{s_0(\alpha-\beta)}\right)}{(\alpha-\beta)^2} - \frac{\beta\left(\alpha\left(s_\xi-s_0\right)+1\right)}{\alpha-\beta} \quad (15)$$

This is the same result, after appropriate adjustment of parameters, as given by Eq. (31) in Laio et al. (2001). The mean saturation excess IET $T_\mu^s[1,1]$ comes from substitution of s_0=s_ξ=1 in Eq. (15):

$$\frac{T_\mu^s[1,1]}{\bar{t}_b} = \frac{\alpha e^{\alpha-\beta}-\beta}{\alpha-\beta} \quad (16)$$

As a result of our more general derivation we can use Eq. (A5), (A13) and (A10) together with n=2, and T_1=$T_\mu^s\left[s_0, s_\xi\right]$, to derive the raw moment T_2. From the relationship between the central moments and the raw moments (see Table A1), the FPT variance is calculated by $T_{\sigma^2}^s\left[s_0, s_\xi\right] = T_2 - T_1^2$. After substitution of s_0=s_ξ=1 we can show the variance of IET arising from the storage threshold, $T_{\sigma^2}^s[1,1]$ is given by:

$$\frac{T_{\sigma^2}^s[1,1]}{\bar{t}_b^2} = \frac{2\alpha\beta e^{\alpha-\beta}(\alpha+\beta+2)}{(\beta-\alpha)^2} + \frac{(\alpha+\beta)\left(\beta^2-\alpha^2 e^{2(\alpha-\beta)}\right)}{(\beta-\alpha)^3} \quad (17)$$

In this paper we do not present the full solution for $T_{\sigma^2}^s\left[s_0, s_\xi\right]$ or the other higher moments as they are rather cumbersome; however complete solutions for the first four moments are provided as supplementary material (http://www.hydrol-earth-syst-sci-discuss.net/3/2853/2006/hessd-3-2853-2006-supplement.pdf). Table 2 summarises the first four central moments of the IET for three limiting cases, as discussed in more detail in the next section.

6 Results and discussion

6.1 Climate controls on threshold storage events

This section discusses the analytical results for the statistical properties of the time between threshold storage events and the statistics of the event magnitudes based on an investigation of three limiting climates: an extremely humid climate with an aridity index $AI=0$ by taking the limit $\alpha \to 0$ of the derived statistics; an extremely arid climate with an aridity index $AI=\infty$ by taking the limit $\beta \to 0$; and an intermediate climate with $AI=1$ by taking the limit $\beta \to \alpha$. The analytical results corresponding to these limiting cases are summarised in Table 2.

6.1.1 Humid climates: $AI=0$

In very humid climates the temporal statistics of saturation excess inter-event times are identical to that of the rainfall (see Table 2). This is because with an excess supply of rainfall and negligible evaporative demand the soil is always saturated. The statistics are consistent with an inter-event time which is exponentially distributed. No filtering takes place as every rainfall event triggers flow and all rainfall becomes saturation excess (see Table 2). The rainfall signal is therefore an excellent indicator of the timing, frequency and magnitude of saturation excess triggered flow events.

6.1.2 Arid climates: $AI=\infty$

The IET statistics of saturation excess events for an arid climate (Table 2) resemble those of the infiltration excess filtering described above (refer to Table 1). The average rate of storage threshold events is scaled by the probability of filling the store completely in a single event i.e. by $P\left[h>w_0\right]=e^{-w_0/\gamma}=e^{-\alpha}$. For example, consider a water repellent soil with a distribution layer which triggers finger flow after a critical water content (Dekker et al., 2001) equivalent to 10 mm of storage. In an extremely arid

climate ($\beta \approx 0$) with a mean rainfall depth per storm of 2 mm ($\alpha=5$), and a mean time between storms $\bar{t}_b=5$ days, the resulting mean and variance of the preferential flow IET is $5e^5$ days and $25e^{10}$ days^2 respectively. Again the statistics are consistent with an IET which is exponentially distributed. The independence of events is maintained because soil moisture is completely depleted before every rainfall event. In this instance a simple filtering of the rainfall, for $h>w_0$, provides a good predictor of the timing, relative frequency and magnitude of storage threshold flow events.

The mean saturation excess magnitude Q_μ is also proportional to the mean storm depth scaled by the probability of filling the store on a single event (see Table 2). However unlike the simple threshold filtering as described by the temporal dynamics the variance of the magnitude of saturation excess events per storm Q_{σ^2} is larger than would be expected for an exponentially distributed random variable with the given mean. We believe this is due to the fact that the statistic includes a large number of zero values where storms do not trigger a threshold storage event. A coefficient of variation of event magnitude $Q_{cv}=\sqrt{2e^{\alpha}-1}$ indicates that in the limit of a very arid climate the relative variability of the magnitude of these events increases with increasing storage capacity and decreasing storm depth (increasing α). For the example described above ($\alpha=5$) the mean, variance and coefficient of variation of event magnitudes are equal to $Q_\mu=0.013$ mm $Q_{\sigma^2}=0.054$ mm^2 and $Q_{cv}=17.2$ respectively.

6.1.3 A balanced climate: $AI=1$

For the case when demand balances supply ($AI=1$), the mean time between storage threshold events is $1+\alpha$ times greater than the mean time between storms $\bar{t}_b$ and the variance is $2\left(\alpha^3+2\alpha^2+2\alpha+1\right)/3$ times greater than the variance of inter-storm times $\bar{t}_b^2$ (see Table 2). To put this into context using the example described above for a water repellent soil i.e. $w_0=10$ mm, $\gamma=2$ mm per storm ($\alpha=5$), and say $E_m=2$ mm/day and $\bar{t}_b=1$ day ($\beta=5$), results in $T_\mu^s[1,1]=6$ days, $T_{\sigma^2}^s[1,1]=124$ days^2, $T_{cv}^s[1,1]=1.86$, $T_\varepsilon^s[1,1]=644$, and $T_\kappa^s[1,1]=17.7$. In comparison the rainfall has $T_\mu^r[1,1]=1$ day,

$T^r_{\sigma^2}[1,1]=1$ day, $T^r_{cv}[1,1]=1$, $T^r_{\varepsilon}[1,1]=2$, and $T^r_{\kappa}[1,1]=6$ (refer to Table 2). The coefficient of variation of saturation excess inter-event times, being greater than 1, is indicative that the process is temporally clustered.

Unlike the filtering that is associated with the infiltration excess runoff generation mechanism described before, the storage threshold filtering changes the form of the probability distribution of inter-event times. Figure 2b shows conceptually how the saturation excess inter-event time pdf changes from an exponential form in very humid climates (the same pdf as the rainfall inter-event time) to a more peaked, fatter tailed distribution at $AI=1$, reverting to an exponentially distributed variable again at $AI=\infty$. Interestingly it can be seen for the parameters chosen that extreme IETs are actually more probable when $AI=1$ than when $AI=\infty$.

Referring again to the IET statistics for $AI=1$ (Table 2), as the storage capacity increases, relative to the supply and demand, (i.e. increasing α) the mean storage threshold IET increases, as does the variance and this increases faster than the square of the mean, which results in an increase in the coefficient of variation. Therefore the clustering of events in time tends to increase with increasing storage capacity. Additionally increasing storage capacity, relative to mean rainfall and evaporation, leads to an increased coefficient of skewness and coefficient of kurtosis indicating a more strongly peaked, fatter tailed pdf. This suggests both an increased likelihood of relatively short IETs (increased peakiness) while at the same time an increased likelihood of much longer IETs (more skewed and fatter tailed). Such behaviour is characteristic of our earlier definition of temporal clustering. For clarity and brevity we restrict further discussion to the first two moments only, allowing us to describe the average IET, the variability as well as the temporal clustering by the coefficient of variation.

The mean and the variance of the event magnitude decrease, and the coefficient of variation increases with increasing storage capacity (larger α), or equal decreases in mean storm depth and mean inter-storm evaporation (see Table 2). For the example described above the mean, variance and coefficient of variation of the event magnitude are equal to $Q_{\mu}=0.33$ mm $Q_{\sigma^2}=1.2$ mm^2 and $Q_{cv}=3.3$ respectively.

6.1.4 All climates $0<AI<\infty$

The statistics for the limiting climates described above indicate that the mean and the variance of the IET tend to increase, and the mean and variance of the event magnitude tend to decrease with increasing aridity. However the variability of event timing relative to the mean ($T^s_{cv}[1,1]$) behaviour tends to peak at intermediate aridity, while the relative variability of event magnitudes continues to increase with increasing aridity. Figures 3 and 4 summarises how the statistics of saturation excess inter-event times and event magnitudes change as a function of aridity for various levels of the demand ratio.

Strong demand (small β) results in a higher mean and variance but a low coefficient of variation of inter-event times and as a result more regular, less clustered events, with a maximum $T^s_{cv}[1,1]$ well into in the arid region (see Fig. 3). Strong demand also results in a higher mean and variance of the event magnitude at the same aridity, but they tend to decrease as the aridity increases (see Fig. 4). While the mean and variance decrease with increasing aridity, the coefficient of variation of the event magnitude increases.

The lower the demand, relative to the storage capacity (larger β), the larger the mean and variance of the IET and the greater the tendency for temporal clustering of events (larger $T^s_{cv}[1,1]$). The tendency for saturation excess events to cluster in time is most pronounced in deep stores when supply equals demand i.e. $AI=1$. This is consistent with the observation by Milly (2001) that as the storage capacity increases the maximum variance in soil moisture tends to peak nearer $AI=1$.

These results are at least qualitatively consistent with observations of decreasing mean annual runoff with aridity (Budyko, 1974) and an increasing coefficient of variation of annual runoff with a reduction in mean annual rainfall (Potter et al., 2005). Temporal clustering has been observed in the flood record (Franks and Kuczera, 2002; Kiem et al., 2003) however this has been attributed to interactions between the Inter-decadal Pacific Oscillation and the El Níno Southern Oscillation changing rainfall patterns. Our

quantification of temporal clustering here however is based upon on a stationary description of climate. We have as yet found no literature quantifying saturation excess in terms of its temporal dynamics with which we can compare to the statistics derived here.

In summary our results suggest the following about threshold storage triggering: In very arid climates the relative variability of the timing of events is low, as is the contribution of saturation excess to the water balance, as evidenced by a low mean event magnitude. However the relative variability of the event magnitude Q_{cv} is high; Saturation excess events in semi-arid environments appear to be prone to high coefficients of variation in both the magnitude of events and the time between events, while contributing a non-negligible proportion of the overall water balance; Sub-humid climates have a large proportion of rainfall converted to runoff. The magnitude of these events occur with a lower Q_{cv} than semi-arid climates and temporal clustering may be a significant feature of the dynamics; In humid climates storage threshold events contribute a significant proportion of the water balance and the variability (relative to the mean) of the timing and magnitude of these events is low.

6.2 Frequency magnitude relationships

It is often the case that we can only observe directly the triggering of events but not the flux. For example the occurrence of soil moisture above a critical value may indicate that macropores are required to have been filled and as a result preferential flow triggered. However, it is typically not possible to measure the flux through either the soil matrix or the macropores, but only relative changes in storage. The timing of triggering and the magnitude of the events however are related to one another through soil moisture storage. In this section we investigate the relationships between the statistics of event timing and event magnitude.

6.2.1 Comparison of means

One would expect that the more frequently threshold storage events occur the greater the contribution of saturation excess to the overall water balance. In fact for the threshold storage model the dimensionless mean saturation excess event magnitude equals the dimensionless mean saturation excess frequency i.e. $Q_\mu/\gamma=\bar{t}_b/T^s_\mu[1,1]$ as shown by comparing Eq. (11) and Eq. (15). This makes physical sense, for example when $T^s_\mu[1,1]=\infty$, Q_μ must be zero, and when $\bar{t}_b=T^s_\mu\left[s_0,1\right]$, Q_μ must equal γ. Noting that $\bar{N}=T^s_\mu[1,1]/\bar{t}_b$ describes the mean number of storms in the IET, it can be shown using Eq. (10) that $Q_\mu/\gamma=\bar{t}_b/T^s_\mu[1,1]$ is equivalent to $E_a=\gamma\left(\bar{N}-1\right)/\bar{N}$. More specifically this indicates that the inputs (rainfall) must be greater than the losses (actual evaporation) in the time between successive events. Intuitively this must be true irrespective the nature of the loss function $L[s]$, however whether such a relationship between mean event magnitude and mean event frequency should hold for more general loss functions $L[s]$ is yet to be shown.

6.2.2 Comparison of relative variability

In addition to the issue of observability mentioned in Sect. 6.2.1 the relationship between the variability of event magnitudes and the variability of the timing of event triggering may have important ecological implications. For example Sher et al. (2004) noted that the temporal variability of resource supply events in arid ecosystems may be as or even more important ecologically than the variability in the magnitude of such events, particularly in semi-arid and arid ecosystems. Here we compare how the coefficient of variation of inter-event times relates to the coefficient of variation of event magnitude in terms of their ratio $T^s_{cv}[1,1]/Q_{cv}$ as a function of aridity (see Fig. 5). For all climates $T^s_{cv}[1,1]\leq Q_{cv}$. In humid climates $T^s_{cv}[1,1]\sim Q_{cv}$ meaning event timing and the magnitude of event per storm are both similarly variable with respect to their means. In very arid climates $T^s_{cv}[1,1]<Q_{cv}$ indicating less variability in event timing relative to its mean in comparison to event magnitude. The ratio approaches a step

function in the limit of a large storage capacity, relative to the climatic forcing i.e. large β (or α not shown), and the step occurs around an aridity index of 1. Mean soil moisture essentially behaves the same way when the storage capacity is large i.e. it is very close to saturation for all $AI<1$ and very close to zero for all $AI>1$. The smaller the storage capacity relative to the climate forcing (small β) the lower the aridity at which $T_{cv}^{s}[1,1]$ and Q_{cv} can be differentiated and the more gradual and smaller the difference with increasing aridity in comparison to larger capacities. Despite increased variability in the timing of saturation excess events for deeper stores for sub-humid and semi-arid environments (see Fig. 3), event magnitude variability increases much more rapidly with increasing aridity and continues to do so for $AI>1$.

In terms of the issue of observability our results suggest that the temporal variability of event triggering may give some understanding of the relative variability of event magnitude in humid climates as they are of a similar magnitude in this region. Based upon the relationship between mean event frequency and mean event magnitude the variance of event magnitude per storm event might even be estimated reasonably. In arid climates $T_{cv}^{s}[1,1]$ is much less than Q_{cv} and tells little about the event magnitude variability but none the less provides a reasonably certain measure (i.e. a standard deviation about the same as the mean) of the variability of event timing. Returning to the hypothesis of Sher et al. (2004), our results suggest that the variability of the timing of potential resource supply events, despite being of long duration on average is actually quite low in comparison to the mean. The temporal variability is also much less than the variability in the magnitude of supply at least on a per storm basis. This suggests that adaptations to cope with temporal variability may be particularly beneficial in arid climates as it may be a reasonably certain (low variability) component of the hydrological variability.

6.3 Relationship between temporal statistics and storage

For some hydrological processes neither the flux nor the triggering are directly observable at the space and time scales at which they occur in the field. This is true in

particular for preferential flow. What is measurable, at least at the point scale, is soil moisture storage. Therefore we explore here first how the temporal statistics relate to the statistics of storage and then the sensitivity of the temporal statistics to the initial storage.

6.3.1 Relationship between temporal statistics and statistics of storage

Figure 6a shows the relationship between the dimensionless mean saturation excess inter-event time $T_{\mu}^{s}[1,1]$ and the mean storage S_{μ} for constant evaporative demand (constant β). This can also be seen in the time series of storage Fig. 6c corresponding to the symbols in Fig. 6a. The mean inter-event time increases nonlinearly as the mean storage decreases, and also increases with increasing storage capacity (increasing values of β). The mean inter-event time is most sensitive to changes in low mean soil moisture. This sensitivity is also high at very high mean soil moisture when the storage capacity is large relative to the climatic forcing (large β).

It is evident by comparing the time series Fig. 6c and Fig. 6a that high mean soil moisture is related to low soil moisture variability and frequent event triggering. Low soil moisture variability is also associated with a low mean soil moisture and infrequent triggering. High variability in soil moisture tends to be associated with intermediate S_{μ} as there is a greater potential for soil moisture fluctuations to explore the entire capacity. This large variability in soil moisture is also associated with high temporal clustering. It can be seen from the relationship between $T_{cv}^{s}[1,1]$ and the variance of storage S_{σ^2} (Fig. 6b) that for a constant evaporative demand (constant β), the maximum $T_{cv}^{s}[1,1]$ occurs when S_{σ^2} is also a maximum. This appears to be true for all but the smallest stores (see $\beta=1$ in Fig. 6b) but in this instance the degree of temporal clustering is low in any case.

6.3.2 The role of initial storage s_0

So far we have largely discussed the controls on the inter-event time, that is the time between successive occurrences of storage at capacity. The analytical derivation of first passage time statistics allows us to determine the climate controls on the statistical properties of the time to trigger saturation excess flow for the first time since an arbitrary initial storage. Figure 1b shows this first passage time as τ_1, the time to reach s=1 for the first time since storage was initially at s_0. If for example we have taken a measurement of storage the FPT statistics $T_x\left[s_0, 1\right]$ can tell us something of the expected value and the variability of the time till the next saturation excess event due to variability in the timing and magnitude of rainfall. Figure 7 shows the effect of initial storage on the mean and the coefficient of variation of the time till the next saturation excess triggering.

It can be seen that the mean first passage time $T_\mu\left[s_0, 1\right]$ decreases as s_0 increases towards saturation and is more sensitive to s_0 at higher soil moisture values. Also, as expected, the mean time till the next event is longer the higher the aridity (compare ratios of α and β in Fig. 7). On the other hand the coefficient of variation of the first passage time $T_{cv}\left[s_0, 1\right]$ increases with increasing initial storage. At low s_0 the more humid the climate the lower $T_{cv}\left[s_0, 1\right]$ but this transitions at higher s_0 such that the more balanced climates and systems with deeper storage capacity relative to the climatic forcing (larger α and β) tend to have a larger $T_{cv}\left[s_0, 1\right]$.

Values of $T_{cv}\left[s_0, 1\right]$ when s_0 is low are $\leq$1. This can be explained for the case of arid climates where the closer s_0 is to zero, as well as being close to S_μ, only extreme rainfall will trigger an event and for reasons discussed in Sect. 6.1.2 event triggering displays similar but scaled statistical properties to the rainfall. The more humid the climate the further away s_0=0 is to S_μ and one would expect a more steady, less variable, increase in storage towards capacity and therefore a lower $T_{cv}\left[s_0, 1\right]$.

On the other hand when a storage threshold flow event has just occurred (s_0=1) the mean time till the next flow event is a minimum and $T_{cv}\left[s_0, 1\right]$ is a maximum. $T_{cv}\left[s_0, 1\right]$

is a measure of our uncertainty, relative to our expected value, of the timing of the next storage threshold event due to our uncertainty in the timing and magnitude of rainfall. This implies that if a saturation excess event has just occurred, while we can expect a second event to occur sooner than at any other time, our ability to predict when that will be, relative to the mean time, is actually at its poorest. The high variability of inter-event times when the initial soil moisture is at saturation we believe is due to the greater potential for both much longer periods between events as a result of the greater potential for drying, as well as a high potential for shorter inter-event times due to the high potential for event triggering when storage is near capacity.

The variability of nonlinear storage dependent hydrological processes seems sensitive to an initial storage near a threshold. Zehe and Blöschl (2004) also found the variability of modelled plot and hillslope scale runoff to be highest when initial soil moisture was at a threshold. In their case they considered a single prescribed rainfall event but multiple realisations of sub-scale spatial variability of initial soil moisture in relation to the spatially averaged initial soil moisture. When the spatially averaged soil moisture was at the threshold between matrix flow and preferential flow the variability of modelled runoff was at its greatest. $T_{cv}\left[s_0, 1\right]$ is a measure of our uncertainty in the timing of the next event due to the randomness of the timing and magnitude of subsequent rainfall events, given an initial storage. Additionally the variability in runoff described by Zehe and Blöschl (2004) is a measure of uncertainty in the magnitude of the event due to an uncertain structure of sub-scale soil moisture. Combining these two results it suggests that the time between two consecutive threshold flow events for which the flux is poorly predictable is itself highly uncertain.

7 Summary and conclusions

Typically in hydrology we consider the transformation of a flux to a flux. Here instead we consider the transformation of event timing to event timing. We have analytically derived statistics of the temporal dynamics of the flow triggering due to a rainfall intensity

threshold and a soil moisture threshold as models for infiltration excess and saturation excess runoff generating mechanisms, respectively. For the saturation excess mechanism though we have gone further to also consider how the temporal dynamics relates to the statistical properties of soil moisture storage and the magnitude of runoff events. The major conclusions are summarised as follows:

- The rainfall intensity threshold produces an inter-event time distribution that is a scaled version of the storm arrival distribution. The scaling factor is related the probability of exceeding the intensity threshold on a single event.
- The soil moisture storage threshold on the other hand leads to temporal clustering of events.
- The mean and the variance of the inter-event time increase with increasing climate aridity however the coefficient of variation of the inter-event time (a measure of the temporal clustering) passes through a maximum which occurs around an aridity index of 1 for systems with a deep storage capacity.
- The mean and the variance of the saturation excess runoff magnitude per storm decrease with increasing aridity, however the coefficient of variation of this event magnitude increases with increasing aridity.
- The dimensionless mean saturation excess event magnitude was found to be equal to the dimensionless mean event frequency.
- The coefficient of variation of saturation excess event magnitude is always greater than or at least equal to the coefficient of variation of the time between saturation excess events. This difference increases with increasing climate aridity.
- High temporal variability of saturation excess events tends to be associated with an intermediate mean and a high variance of soil moisture.

- When beginning with an arbitrary initial soil moisture the expected time till the next event is a minimum but the variability relative to that value is a maximum when initial storage is at the threshold.

We consider our results to be potentially limited to relatively small spatial scales where such thresholds have the greatest potential to be expressed as discrete events. At larger spatial scales the effect of spatio-temporal rainfall and runoff is expected to dominate runoff dynamics although nonlinear and threshold processes have been shown to strongly influence the flood frequency curve at a range of spatial scales (Blöschl and Sivapalan, 1997). Additionally climate is subject to long term variability and change. Future research should therefore consider how spatio-temporal rainfall and climate fluctuations impact the temporal dynamics as well as its relationships to runoff magnitude and storage within the landscape.

Appendix A Derivation of saturation excess temporal statistics

The integral equation for the pdf of first passage times, g_T, for a deterministic process interrupted by bursts of instantaneous Poisson noise (a shot noise process) was given by (Laio et al., 2001) as:

$$\frac{\partial g\left(t|s_0\right)}{\partial t} = -L\left[s_0\right]\frac{\partial g\left(t|s_0\right)}{\partial s_0} - \lambda\, g\left(t|s_0\right) + \lambda\int_{s_0}^{s_\xi} f_H\left[z - s_0\right]\, g\left(t|z\right)\, \mathrm{d}z \qquad \text{(A1)}$$

where f_H is the pdf of storm depths, z is a dummy variable of integration, s_ξ is an arbitrary threshold soil moisture, and $\lambda = 1/\bar{t}_b$ the mean storm frequency. The raw moments of the first passage time are by definition:

$$T_n^s\left[s_0, s_\xi\right] = \int_0^\infty t^n g_T\left(t|s_0\right)\, \mathrm{d}t \qquad \text{(A2)}$$

Equation (A2) motivates us to generalise the derivation to higher order moments by multiplying Eq. (A1) by t^n (instead of t to just get the mean as done by Laio et al. (2001). So multiplying Eq. (A1) by t^n, assuming storm depths are exponentially distributed and integrating by parts the time derivative and substituting $T_n^s\left[s_0, s_\xi\right]$, results in the following integro-differential equation for the first passage time moments:

$$-nT_{n-1}^s\left[s_0, s_\xi\right] = -L\left[s_0\right]\frac{\mathrm{d}T_n^s\left[s_0, s_\xi\right]}{\mathrm{d}s_0} - \lambda T_n^s\left[s_0, s_\xi\right] + \frac{\lambda}{\gamma}\int_{s_0}^{s_\xi} e^{-(z-s_0)/\gamma}T_n^s\left[z, s_\xi\right]\,\mathrm{d}z \tag{A3}$$

Integrating by parts the integral term in Eq. (A3), differentiating the entire equation with respect to s_0, and substituting for the integral term by rearranging Eq. (A3), leads to a second order ordinary differential equation for the first passage time moments T_n^s :

$$L\left[s_0\right]\frac{\mathrm{d}^2T_n^s}{\mathrm{d}s_0^2} + \frac{\mathrm{d}T_n^s}{\mathrm{d}s_0}\left(\frac{\mathrm{d}L\left[s_0\right]}{\mathrm{d}s_0} - \frac{L\left[s_0\right]}{\gamma} + \lambda\right) = \frac{\mathrm{d}T_{n-1}^s}{\mathrm{d}s_0} - \frac{n}{\gamma}T_{n-1}^s \tag{A4}$$

The general solution to Eq. (A4) is given by:

$$T_n^s[s_0, s_\xi] = C_2 + C_1\int_1^{s_0} B_1\left[w, 1\right]\mathrm{d}w + \int_1^{s_0} B_2\left[w, 1\right]\mathrm{d}w \tag{A5}$$

where

$$\ln(B_1[a, b]) = \alpha\left(a - 1\right) + \int_a^b \frac{1}{L[x]}\left(\lambda + \frac{\mathrm{d}L[x]}{\mathrm{d}x}\right)\mathrm{d}x \tag{A6}$$

$$B_2\left[w, 1\right] = -B_1[w, 1]\int_w^1 \frac{nB_1\left[1, y\right]}{L[y]}\left(\alpha T_{n-1}\left[y, s_\xi\right] - \frac{\mathrm{d}T_{n-1}\left[y, s_\xi\right]}{\mathrm{d}y}\right)\mathrm{d}y \tag{A7}$$

and w, x and y are dummy variables of integration. Two boundary conditions are required to solve for the coefficients C_1 and C_2. The first boundary condition is derived

when the process begins at the threshold (Laio et al., 2001; Masoliver, 1987) and is obtained by substituting $s_0{=}s_\xi$ in Eq. (A3) to get:

$$L\left[s_0\right]\frac{\mathrm{d}T_n^s\left[s_0, s_\xi\right]}{\mathrm{d}s_0}\bigg|_{s_0=s_\xi} = nT_{n-1}^s\left[s_\xi, s_\xi\right] + \lambda T_n^s\left[s_\xi, s_\xi\right]] \tag{A8}$$

The second boundary condition is required to describe the time to reach the threshold having begun at the lower boundary and is obtained from substitution of $s_0{=}0$ in Eq. (A3) (Laio et al., 2001; Masoliver, 1987) resulting in:

$$-nT_{n-1}^s\left[0, s_\xi\right] = -\lambda T_n^s\left[0, s_\xi\right] + \frac{\lambda}{\gamma}\int_0^{s_\xi} e^{-(z-s_0)/\gamma}T_n^s\left[z, s_\xi\right]\,\mathrm{d}z \tag{A9}$$

The coefficient C_1 can be obtained by differentiating Eq. (A5) with respect to s_0, inserting this into Eq. (A8), substituting $s_0{=}s_\xi$ and then solving for C_1 , which is dependent upon C_2. Substituting Eq. (A5) in the second boundary condition Eq. (A9) gives a second equation for C_1 also dependent upon C_2. Equating these two expressions and solving for C_2 gives:

$$C_2 = \left(\frac{B_3[3] + nT_{n-1}[0, s_\xi]/\lambda}{B_3[1]} - \frac{B_4[3] - nT_{n-1}[s_\xi, s_\xi]}{B_4[1]}\right) \div \left(\frac{e^{-\alpha s_\xi}}{B_3[1]} + \frac{\lambda}{B_4[1]}\right) \tag{A10}$$

where

$$B_4[A] = L[s_\xi]B_A[s_\xi, 1] - \lambda\int_{s_0}^1 B_A[w, 1]\mathrm{d}w \tag{A11}$$

and

$$B_3[A] = \int_0^{s_\xi} \alpha e^{-z\alpha}\int_1^z B_A[w, 1]\mathrm{d}w\,\mathrm{d}z + \int_0^1 B_A[w, 1]\mathrm{d}w \tag{A12}$$

The subscript A is a reference to B_A as given by Eq. (A6) or Eq. (A7). Substituting Eq. (A10) into one of the original expressions for C_1 gives:

$$C_1 = -\left(nT_{n-1}\left[s_{\xi}, s_{\xi}\right] - e^{\alpha s_{\xi}}\left(nT_{n-1}\left[0, s_{\xi}\right] + \lambda B_3\left[3\right]\right) - B_4\left[3\right]\right) \div \left(\lambda e^{\alpha s_{\xi}} B_3\left[1\right] + B_4\left[1\right]\right) \tag{A13}$$

The central moments can be derived from these raw moments using the relationships described in Table A1 and as discussed in Sect. 5.2.

Appendix B List of Symbols

Symbol	Description	Units
Soil parameters		
I_{ξ}	Infiltration capacity	LT^{-1}
w_0	Storage capacity	L
s	Normalised soil moisture storage	–
s_0	Initial soil moisture	–
s_{ξ}	Threshold soil moisture	–
Climate parameters		
h	Storm depth	L
γ	Mean storm depth	L
t_b	Inter storm duration	T
$\bar{t}_b$	Mean inter-storm duration (λ^{-1})	T
E_m	Potential evaporation	LT^{-1}
$I_{\max}$	Max within storm rainfall intensity	LT^{-1}
ς	Mean $I_{\max}$	LT^{-1}
Probability terms		
f_X	Probability density	X^{-1}
g_T	First passage time probability density	T^{-1}
$P[\ ]$	Probability	–
μ	Mean	X [a]
σ	Standard deviation	X [a]
σ^2	Variance	X^2 [a]

[a] Units X correspond to the random variable

Symbol	Description	Units
Probability terms		
cv	Coefficient of variation	–
ε	Coefficient of skewness	–
κ	Coefficient of kurtosis	–
Dimensionless hydrological parameters and statistics		
α	Supply ratio	–
β	Demand ratio	–
AI	Aridity index	–
E_a	Mean actual evaporation	L
$\bar{N}$	Mean number of storms in the IET	–
Q_x	Saturation excess event magnitude statistic	[a]
S_x	Soil moisture storage statistic	–
$T_x^I\left[I_\xi\right]$	Infiltration excess IET statistic	[a]
T_x^r	Storm IET statistic	[a]
$T_x^s\left[s_0, s_\xi\right]$	Statistic of the time to reach s_ξ since an initial soil moisture s_0	[b]

[a] Units correspond to Q_μ [L], Q_{σ^2}[L^2], and Q_{cv} [–].

[b] Units correspond to T_μ [T], T_{σ^2}[T^2], T_{cv} [–], T_ε [–], and T_κ [–].

Acknowledgements. The research was made possible by an Australia Postgraduate Award (Industry) from the Australian Research Council in conjunction with the Centre for Groundwater Studies. In addition G. S. McGrath would like to thank Amilcare Porporato for his assistance and comments on an early manuscript.

References

Bauters, T.: Soil water content dependent wetting front characteristics in sands., J. Hydrol., 231–232, 244–254, 2000. 2856

Beven, K. and Germann, P.: Macropores and water flow in soils, Water Resour. Res., 18, 1311–1325, 1982. 2855, 2856

Blöschl, G. and Sivapalan, M.: Process controls on regional flood frequency: Coefficient of variation and basin scale, Water Resour. Res., 33, 2967–2980, 1997. 2878

Bresler, E. and Dagan, G.: Convective and pore scale dispersive solute transport in unsaturated heterogeneous fields, Water Resour. Res., 17, 1683–1693, 1982. 2855

Budyko, M.: Climate and Life., Academic Press, New York, 1974. 2870

Crockford, R. and Richardson, D.: Partitioning of rainfall into throughfall, stemflow and interception: effect of forest type, groundcover and climate, Hydrol. Process., 14, 2903–2920, 2000. 2855, 2856

Dekker, L. W., Doerr, S. H., Oostindie, K., Ziogas, A. K., and Ritsema, C. J.: Water repellency and critical soil water content in a dune sand, Soil Sci. Soc. Am. J., 65, 1667–1674, 2001. 2856, 2867

Dunne, T.: Field studies of hillslope flow processes, in: Hillslope Hydrology, edited by: Kirkby, M. J., John Wiley and Sons, Chichester, West Sussex, UK, 1978. 2855

Fitzjohn, C., Ternan, J., and Williams, A.: Soil moisture variability in a semi-arid gully catchment: implications for runoff and erosion control, Catena, 32, 55–70, 1998. 2855

Franks, S. W. and Kuczera, G.: Flood frequency analysis: Evidence and implications of secular climate variability, New South Wales, Water Resour. Res., 38, 1062, doi:10.1029/2001WR000232, 2002. 2870

Godano, C., Alonzo, M., and Vildaro, G.: Multifractal approach to time clustering of earthquakes: Application to Mt. Vesuvio seismicity, Pure and Appl. Geophys., 149, 375–390, 1997. 2859

Haria, A. H., Johnson, A. C., Bell, J. P., and Batchelor, C. H.: Water-movement and isoproturon behavior in a drained heavy clay soil .1. Preferential flow processes, J. Hydrol., 163, 203–216, 1994. 2856

Heppell, C. M., Worrall, F., Burt, T. P., and Williams, R. J.: A classification of drainage and macropore flow in an agricultural catchment, Hydrol. Process., 16, 27–46, 2002. 2856, 2860

Jarvis, N. J., Stahli, M., Bergstrom, L., and Johnsson, H.: Simulation of dichlorprop and bentazon leaching in soils of contrasting texture using the macro model., J. Environ. Sci. Health A, 29, 1255–12 770, 1994. 2855

Kiem, A. S., Franks, S. W., and Kuczera, G.: Multi-decadal variability of flood risk, Geophys. Res. Let., 30, 1035, doi:10.1029/2002GL015992, 2003. 2870

Kohler, A., Abbaspour, K. C., Fritsch, M., and Schulin, R.: Using simple bucket models to analyze solute export to subsurface drains by preferential flow, Vadose Zone J., 2, 68–75, 2003. 2856, 2859

Kung, K.-J.: Preferential flow in a sandy vadose zone, 2 : Mechanisms and implications., Geoderma, 22, 59–71., 1990. 2856

Laio, F., Porporato, A., Ridolfi, L., and Rodriguez-Iturbe, I.: Mean first passage times of processes driven by white shot noise, Physical Rev. E, 6303, 2001. 2865, 2866, 2878, 2879, 2880

Masoliver, J.: 1st-Passage times for non-Markovian processes – Shot noise, Physical Rev. A, 35, 3918–3928, 1987. 2865, 2880

Milly, P. C. D.: An analytic solution of the stochastic storage problem applicable to soil-water, Water Resour. Res., 29, 3755–3758, 1993. 2857, 2861, 2862, 2863, 2864, 2865

Milly, P. C. D.: Climate, interseasonal storage of soil-water, and the annual water-balance, Adv. Water Resour., 17, 19–24, 1994. 2861

Milly, P. C. D.: A minimalist probabilistic description of root zone soil water, Water Resour. Res., 37, 457–463, 2001. 2857, 2863, 2865, 2870

Minasny, B. and McBratney, A. B.: Uncertainty analysis for pedotransfer functions, Europ. J. Soil Sci., 53, 417–429, 2002. 2855

Mosley, M.: Streamflow generation in a forested watershed., Water Resour. Res., 15, 795–806, 1976. 2856

Papoulis, A.: Probability, Random Variables and Stochastic Processes, 3rd ed., McGraw-Hill, New York, 2001. 2858, 2859, 2864

Parlange, J.-Y. and Hill, D.: Theoretical analysis of wetting front instability in soils., Soil Sci., 02, 236–239., 1976. 2855

Potter, N. J., Zhang, L., Milly, P. C. D., McMahon, T. A., and Jakeman, A. J.: Effects of rainfall seasonality and soil moisture capacity on mean annual water balance for Australian catchments, Water Resour. Res., 41, W06007, doi:10.1029/2004WR003697, 2005. 2870

Ridolfi, L., D'Odorico, P., Porporato, A., and Rodriguez-Iturbe, I.: Duration and frequency of water stress in vegetation: An analytical model, Water Resour. Res., 36, 2297–2307, 2000. 2865

Rodriguez-Iturbe, I. and Isham, V.: Some models for rainfall based on stochastic point processes, Proc. Royal Soc. London Ser. A – Math. Phys. Eng. Sci., 410, 269–288, 1987. 2857

Rodriguez-Iturbe, I., Porporato, A., Ridolfi, L., Isham, V., and Cox, D. R.: Probabilistic modelling of water balance at a point: the role of climate, soil and vegetation, Proc. Royal Soc. London Ser. A - Math. Phys. Eng. Sci., 455, 3789–3805, 1999. 2857, 2860

Roth, K. and Jury, W. A.: Modeling the transport of solutes to groundwater using transfer-functions, J. Environ. Qual., 22, 487–493, 1993. 2855

Savenije, H. G.: The importance of interception and why we should delete the term evapotranspiration from our vocabulary, Hydrol. Process., 18, 1507–1511, 2004. 2855

Sher, A., Goldberg, D., and Novoplansky, A.: The effect of mean and variance in resource supply on survival of annuals from Mediterranean and desert environments, Oecologica, 141, 353–362, 2004. 2872, 2873

Simunek, J., Jarvis, N. J., van Genuchten, M. T., and Gardenas, A.: Review and comparison of models for describing non-equilibrium and preferential flow and transport in the vadose zone, J. Hydrol., 272, 14–35, 2003. 2856

Struthers, I., Sivapalan, M., and Hinz, C.: Conceptual examination of the influence of climate upon water balance of an open-fractured soil. I. Individual storm response, Adv. Water Resour., in press, 2006a. 2856

Struthers, I., Sivapalan, M., and Hinz, C.: Conceptual examination of the influence of climate upon water balance of an open-fractured soil. II. Long term response to a population of storms, Adv. Water Resour., in press, 2006b. 2856

Teich, M., Heneghan, C., Lowen, S., Ozaki, T., and Kaplan, E.: Fractal character of the neural spike train in the visual system of the cat, J. Opt. Soc. Am. A, 14, 529–545, 1997. 2859

Tromp-van Meerveld, H. and McDonnell, J.: Threshold relations in subsurface stormflow 1. A 147 storm analysis of the Panola hillslope, Water Resour. Res., 42, W02410,

doi:10.1029/2004WR003778, 2006. 2856

Uchida, T., van Meerveld, I. T., and McDonnell, J.: The role of lateral pipe flow in hillslope outflow response: an intercomparison of non-linear hillslope response, J. Hydrol., 311, 117–133, 2005. 2856

Wang, Z., Feyen, J., and Ritsema, C.: Susceptibility and predictability of conditions for preferential flow, Water Resour. Res., 34, 2183–2190, 1998. 2856

Whipkey, R.: Subsurface stormflow from forested slopes., Bull. Int. Assoc. Sci. Hydrol., 10, 74–85, 1965. 2855, 2856

Wood, M. A., Simpson, P. M., Stambler, B. S., Herre, J. M., Bernstein, R. C., and Ellenbogen, K. A.: Long-term temporal patterns of ventricular tachyarrhythmias, Circulation, 91, 2371–2377, 1995. 2859

Zak, S. K. and Beven, K. J.: Equifinality, sensitivity and predictive uncertainty in the estimation of critical loads, Sci. Total Environ., 236, 191–214, 1999. 2855

Zehe, E. and Blöschl, G. N.: Predictability of hydrologic response at the plot and catchment scales: Role of initial conditions, Water Resour. Res., 40, W10202, doi:10.1029/2003WR002869, 2004. 2876

Zeng, N., Shuttleworth, J., and Gash, J.: Influence of temporal variability of rainfall on interception loss. Part I. Point analysis, J. Hydrol., 228, 228–241, 2000. 2856

Table 1. Storm and infiltration excess inter-event statistics.

Statistic	Storm	Infiltration excess
T_{μ}	$\bar{t}_b$	$\bar{t}_b\, e^{I_\xi/\zeta}$
T_{σ^2}	$\bar{t}_b^2$	$\left(\bar{t}_b\, e^{I_\xi/\zeta}\right)^2$
T_{cv}	1	1
T_{ε}	2	2
T_{κ}	6	6

Table 2. Summary statistics of the saturation excess inter-event times and event magnitudes in three limiting climates.

Statistic	Rainfall	Humid $AI=0$	Intermediate $AI=1$	Arid $AI=\infty$
$T^s_\mu[1,1]$	$\bar{t}_b$	$\bar{t}_b$	$\bar{t}_b\,(1+\alpha)$	$\bar{t}_b\,e^\alpha$
$T^s_{\sigma^2}[1,1]$	$\bar{t}_b^2$	$\bar{t}_b^2$	$\frac{2}{3}\left(\alpha^3+2\alpha^2+2\alpha+1\right)\bar{t}_b^2$	$\left(\bar{t}_b e^\alpha\right)^2$
$T^s_{cv}[1,1]$	1	1	$\frac{\sqrt{3}}{\sqrt{2}}\frac{\sqrt{\alpha^3+2\alpha^2+2\alpha+1}}{1+\alpha}\geq 1$	1
$T^s_\varepsilon[1,1]$	2	2	$\frac{\sqrt{3}\left(4\alpha^5+20\alpha^4+40\alpha^3+45\alpha^2+30\alpha+10\right)}{5\sqrt{2\alpha(\alpha(\alpha+3)+3)+3}}\geq 2$	2
$T^s_\kappa[1,1]$	6	6	$\frac{B_1\alpha^7+B_2\alpha^6+B_3\alpha^5+B_4\alpha^4+B_5\alpha^3+B_6\alpha^2+B_7\alpha+B_8}{35(2\alpha(\alpha(\alpha+3)+3)+3)^2}-3\geq 6$ [a]	6
Q_μ	γ	γ	$\frac{\gamma}{1+\alpha}$	$\frac{\gamma}{e^\alpha}$
Q_{σ^2}	γ^2	γ^2	$\frac{(1+2\alpha)}{(1+\alpha)^2}\gamma^2$	$\frac{2e^\alpha-1}{e^{2\alpha}}\gamma^2$
Q_{cv}	1	1	$\sqrt{1+2\alpha}$	$\sqrt{2e^\alpha-1}$

[a] Constants B_i are given by $B_1=408$, $B_2=3276$, $B_3=11\,214$, $B_4=22\,050$, $B_5=27\,720$, $B_6=22\,680$, $B_7=11\,340$, $B_8=2835$.

Table A1. Relationships between raw and central moments.

Central moment	Relation to raw moments
Mean	$T_\mu=T_1$
Variance	$T_{\sigma^2}=T_2-T_1^2$
Coefficient of skewness	$T_\varepsilon=\frac{T_3-3T_1T_2+2T_1^3}{\left(T_2-T_1^2\right)^{\frac{3}{2}}}$
Kurtosis excess	$T_\kappa=\frac{T_4-4T_1T_3+6T_1^2T_2-3T_1^4}{\left(T_2-T_1^2\right)^2}-3$

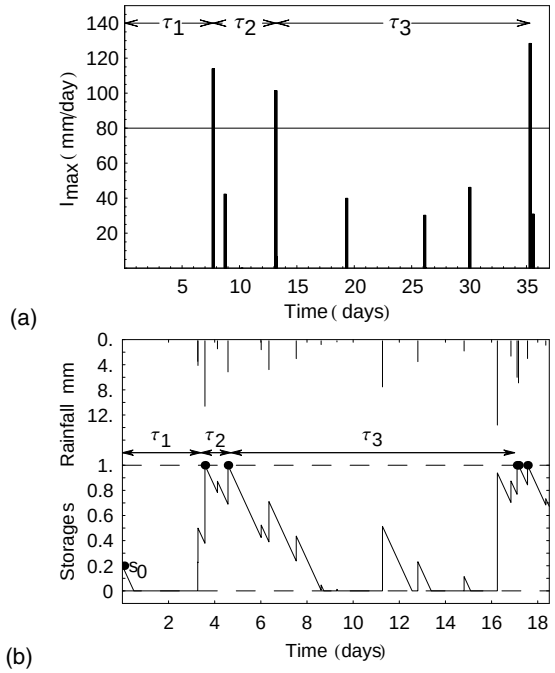

Fig. 1. Definition of the more general first passage time τ_1 and the inter-event time τ_2 and τ_3 for **(a)** a threshold rainfall intensity infiltration excess trigger, where in this example within storm rainfall intensities above the soils infiltration capacity I_ξ=80 mm/day trigger flow; and **(b)** a storage threshold triggered flow, occurring when s=1. s_0 denotes the initial soil moisture.

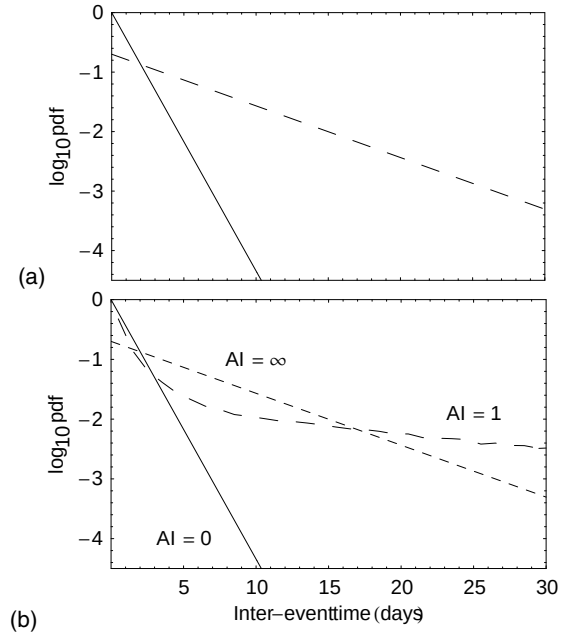

Fig. 2. Conceptual description of the relationship between the rainfall inter-event time (IET) probability density (pdf) and the IET pdf for **(a)** infiltration excess and **(b)** saturation excess. For (a) the dashing corresponds to rainfall (solid) and infiltration-excess (dashed) with I_ξ/ς=5 and $\bar{t}_b$=1 day. For (b) dashing corresponds to rainfall (continuous), an aridity index AI=0 (also continuous), AI=1 (large dashes) and an AI=∞ (small dashes) with $\bar{t}_b$=1 day, and α=5 . Inter-event time pdf estimated at AI=1 from a continuous simulation of 10^5 saturation excess events using Eq. (5).

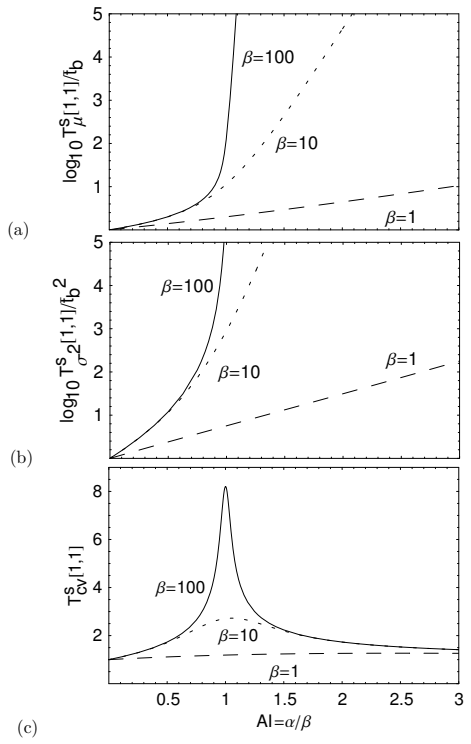

Fig. 3. Variation of statistics of the storage threshold inter-event time with aridity index showing **(a)** mean $T^s_\mu[1,1]$ **(b)** variance $T^s_{\sigma^2}[1,1]$ and **(c)** coefficient of variation $T^s_{cv}[1,1]$ for constant β=1, 10, and 100 (dashed, dotted and continuous respectively).

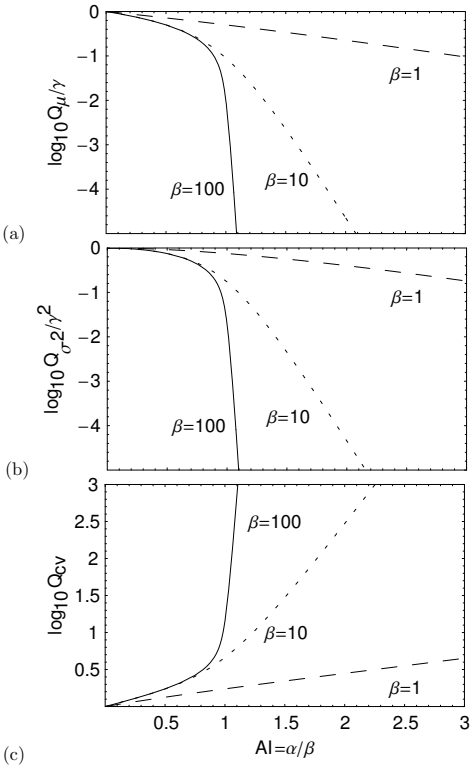

Fig. 4. Variation of statistics of the storage threshold magnitude with aridity index showing **(a)** mean Q_μ **(b)** variance Q_{σ^2} and **(c)** coefficient of variation Q_{cv} for constant β=1, 10, and 100 (dashed, dotted and continuous respectively).

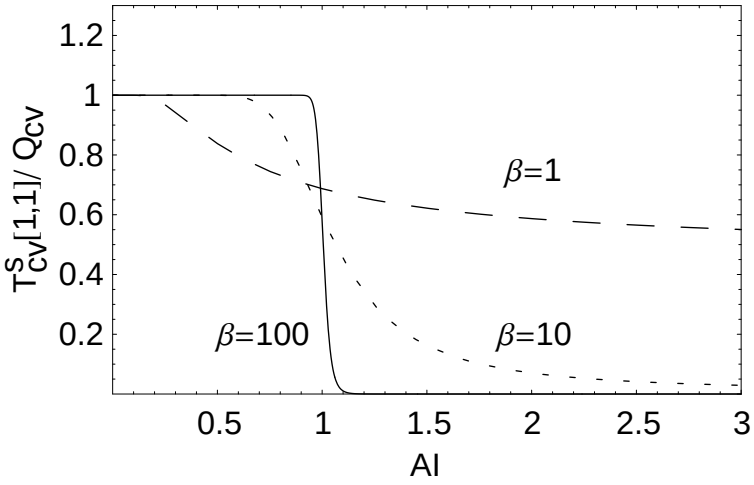

Fig. 5. Ratio of the coefficient of variation of event timing T_{cv} [1, 1] and the coefficient of variation of the event magnitude Q_{cv} as a function of aridity. Dashing corresponds to constant β=1 (large dashed), β=10 (dotted) and β=100 (continuous).

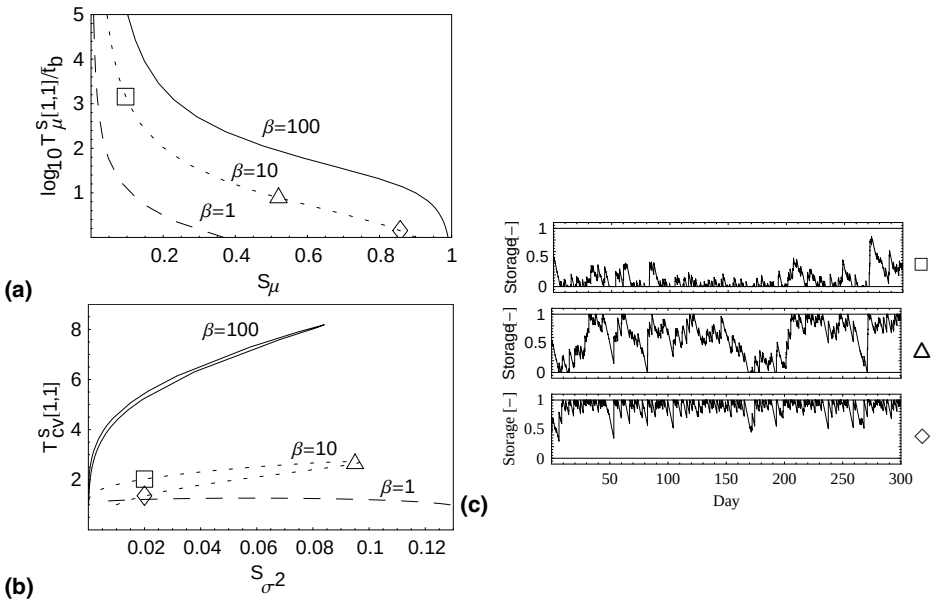

Fig. 6. Relationship between soil moisture storage and the temporal dynamics showing **(a)** Mean inter-event time T^s_μ [1, 1] as a function of mean soil moisture S_μ; **(b)** Coefficient of variation of the inter-event time T^s_{cv} [1, 1] as a function of the variance of soil moisture S_{σ^2}; and **(c)** Soil moisture time series corresponding to symbols in (a) and (b). Dashing corresponds to constant β=1 (large dashed), β=10 (dotted) and β=100 (continuous). Time series generated as described in Sect. 5.1 with $\bar{t}_b$=1 day, E_m=0.5 mm/day, w_0=5 mm and γ=0.307 mm (□), γ=0.536 mm (△), and γ=1.66 mm (◇).

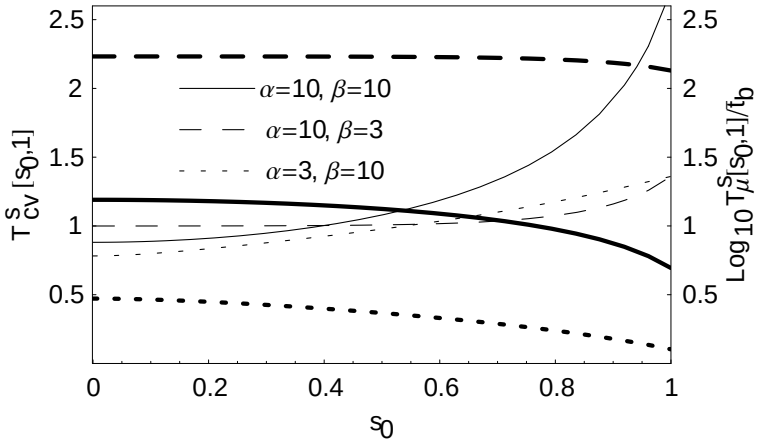

Fig. 7. First passage time statistics vs. the initial soil moisture s_0. Coefficient of variation $T_{cv}[s_0, 1]$ (thin lines) and the mean $T_\mu[s_0, 1]$ (thick lines) of the time to reach s=1 since an initial soil moisture s_0.